Phase gap in pseudoternary $R_{1-y}R'_yMn_2X_{2-x}X'_x$ compounds

J. L. Wang,[1,2,3] S. J. Kennedy,[1,*] S. J. Campbell,[2] M. Hofmann,[4] and S. X. Dou[3]

[1]*Bragg Institute, Australian Nuclear Science and Technology Organisation, Lucas Heights, NSW 2234, Australia*

[2]*School of Physical, Environmental, and Mathematical Sciences, University of New South Wales, Canberra, ACT 2600, Australia*

[3]*Institute for Superconductivity and Electronic Materials, University of Wollongong, Wollongong, NSW 2522, Australia*

[4]*Forschungs-Neutronenquelle Heinz Maier-Leibnitz (FRM-II), Technische Universität München, 85747 Garching, Germany*

(Received 15 February 2012; revised manuscript received 29 June 2012; published 4 March 2013)

Our neutron diffraction investigation of $PrMn_2Ge_{2-x}Si_x$ reveals a clear separation into two magnetic phases, canted ferromagnetic (Fmc) and antiferromagnetic (AFmc), between $x = 1.0$ and 1.2 and a commensurate phase gap in the lattice, due to magnetostrictive distortion. This remarkable magnetoelastic phenomenon is driven by a nonuniform atomic distribution on the X site which in turn produces subtle variations in the local lattice and abrupt changes in the Mn-Mn magnetic exchange interaction. Our results show that coexistence of Fmc and AFmc phases depends on lattice parameter, chemical pressure from the rare-earth and metalloid sites, and local lattice strain distributions. We demonstrate that these magnetostructural correlations act across the entire family of $R_{1-y}R'_yMn_2X_{2-x}X'_x$ compounds.

DOI: 10.1103/PhysRevB.87.104401 PACS number(s): 75.30.Kz, 61.05.F−, 71.20.Eh, 74.62.−c

Ternary rare-earth compounds RMn_2X_2 with X = Si or Ge crystallize in the body-centered tetragonal $ThCr_2Si_2$ type structure with the R, Mn, and X atoms stacked in layers along the c axis in the sequence -R-X-Mn-X-.[1] The family includes all rare-earth elements and yttrium (amounting to thirty compounds) as well as a vast array of pseudoternaries of types $R_{1-y}R'_yMn_2X_2$,[2–10] $RMn_{2-x}T_xX_2$,[11–13] and $RMn_2X_{2-x}X'_x$.[13–16] In most cases with high Mn concentration, the Mn atoms order antiferromagnetically well above room temperature, and some of the rare-earth elements also develop long-range ferromagnetic order at lower temperature. The nature of magnetic order can be ferro-, antiferro-, or ferrimagnetic, and may be commensurate or incommensurate with the lattice, and the axial and planar components appear to develop almost independently of each other. One consistent feature across the complex array of magnetic states is the strong dependence of the magnetic exchange interactions on intraplanar Mn-Mn distances and, to a lesser extent, on interplanar Mn-Mn distances.[2,17–19] It has been frequently noted that the critical intraplanar Mn-Mn distance between ferromagnetic and antiferromagnetic order of the axial component lies around 2.86 Å (average distance). However, significant variation in critical distance is seen for different compositions, so clearly other critical factors (such as electron density distributions and localized strain fields) must be at play. The intriguing magnetic behavior of RMn_2X_2 compounds has attracted sustained interest by many research teams for a period of more than forty years, over which time discontinuous magnetoelastic distortions have also been found to coincide with some of the magnetic structure transitions.

Arguably the most instructive members of the family are the pseudoternaries. Some of these compounds display coexistence of two magnetic phases: canted antiferromagnetic (AFmc) and ferromagnetic (Fmc), over a range of composition and temperature. Since the first report of this phase coexistence in $La_{1-y}Y_yMn_2Si_2$,[6] other observations have been published.[7,8,16] However, to date no explanation of the critical interatomic correlations associated with the boundary between AFmc and Fmc phases or of the origin of the two phase region has been provided. The pseudoternary series $PrMn_2Ge_{2-x}Si_x$ is ideal for investigation of these two issues, since it possesses an extended region of two-phase character.

Magnetic structures of $PrMn_2Ge_2$[15,20–22] and $PrMn_2Si_2$[5] have been well reported[2,5,8,23] and will not be described here. Suffice to note that $PrMn_2Ge_2$ displays Fmc order and that $PrMn_2Si_2$ displays AFmc order below room temperature.

Here we report our findings on pseudoternary $PrMn_2Ge_{2-x}Si_x$, in which we observe a region where Fmc and AFmc phases coexist, with coupled magnetoelastic response such that structural phase separation occurs. This enables us to draw fresh insights into the physical nature of this family of compounds, which we have then generalized to describe the characteristics of the two-phase region in all pseudoternaries of RMn_2X_2 in terms of the valence state of the rare-earth ion, the size of the X ion, and the level of disorder introduced by a solid solution on the R or X site.

$PrMn_2Ge_{2-x}Si_x$ alloys were prepared as described previously.[2,13,16] Magnetization and differential scanning calorimetry (DSC) were used to identify magnetic phase transitions[24] revealing up to five magnetic transitions: Pr site Curie temperature (T_C^{Pr}), critical temperature for incommensurate canted ferromagnetism ($T_{c/c}$), Néel temperature of the axial component of antiferromagnetism (T_N^{inter}), Curie temperature of the axial component of ferromagnetism (T_C^{inter}), and Néel temperature (T_N^{intra}) for planar antiferromagnetism (known as AFl).[2,13]

Neutron diffraction patterns were collected on the E6 diffractometer (BENSC, Berlin), and the Wombat diffractometer (OPAL, Lucas Heights). Structural and magnetic parameters and the proportion of Fmc and AFmc phases were extracted from Rietveld refinements[25] of the neutron diffraction patterns.[24]

Fmc and AFmc phases coexist for $x = 1$ and 1.2, whereas all other samples are single phase. The temperature dependence of the lattice parameters for $x = 1$ and $x = 1.2$ are shown in Fig. 1, along with phase fractions in the two-phase region. For $x = 1$, Fmc and AFmc magnetic phases coexist from ~200 K to T_C^{Pr}. Coexistence extends below T_C^{Pr} only in the

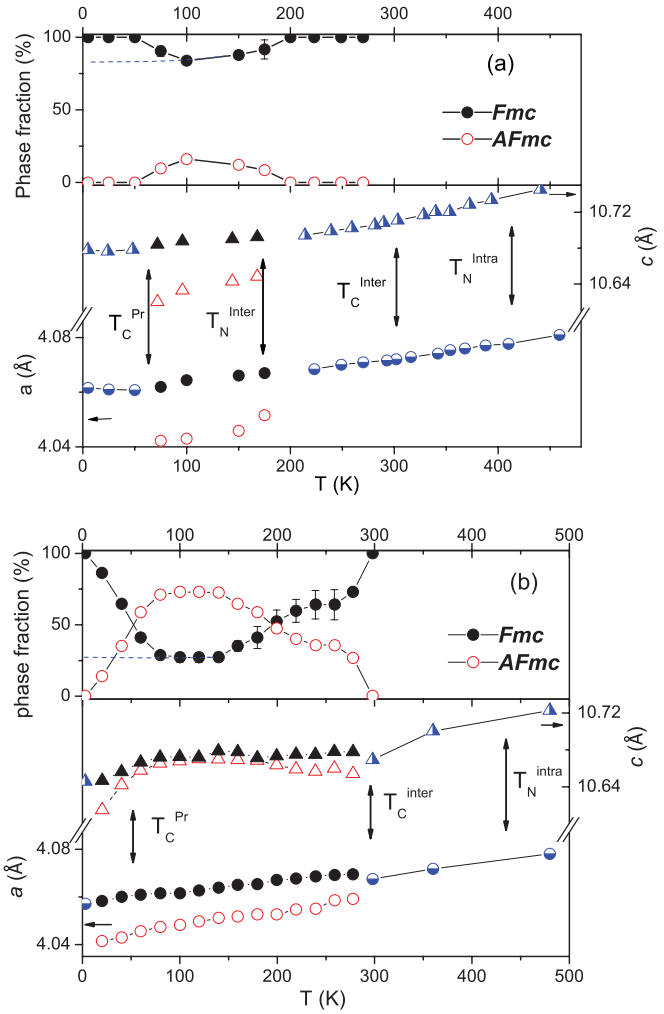

FIG. 1. (Color online) Temperature dependencies of the fractions of the Fmc and AFmc phases and the lattice parameters for (a) $PrMn_2Ge_{1.0}Si_{1.0}$ and (b) $PrMn_2Ge_{0.8}Si_{1.2}$. Solid symbols show the Fmc state, open symbols the AFmc state with the single phase shown by half-filled symbols.

$x = 1.2$ sample. Figure 1 also illustrates the spontaneous magnetostriction which typifies the appearance of Fmc and AFmc ordering in RMn_2X_2 compounds. The transition from intralayer antiferromagnetic (AFl) to Fmc produces a positive spontaneous magnetostriction along the a axis (+0.07%), while the transition from AFl to AFmc produces an even stronger negative spontaneous magnetostriction along the a axis (−0.22%). As far as we can ascertain from neutron diffraction the magnetostriction in both cases is isotropic; i.e., the change in the c-axis dimension is the same as the change in the a-b plane. Thus an induced transition between Fmc and AFmc could produce a linear magnetostriction of ∼0.30% (by comparison, the induced linear magnetostriction in Terfenol-D is 0.16%[26]).

Figure 2 is the magnetic phase diagram for $PrMn_2Ge_{2-x}Si_x$ derived from our results. The majority of the phase boundary lines are well defined by the available data points apart from the Fmc to Fmi phase boundary where extrapolation is indicated by a dotted line.

The shaded area defines the region of coexistence of Fmc and AFmc phases. The boundaries were calculated by linear combination of the observed phase fractions for $x = 1$ and $x = 1.2$ using Eqs. (1)–(3), assuming that at any given temperature, the two-phase region is described by a combination of two phases, each at the limiting concentration of that phase. Hence, we define $x_c^{\mathrm{Fmc}}(T)$ and $x_c^{\mathrm{AFmc}}(T)$ as the critical concentration of the Fmc and AFmc phase at temperature T, respectively, and $p_n(T)$ as the observed fraction of the Fmc phase for nominal Si concentration (x_n). Then $1 - p_n(T)$ is the observed fraction of the AFmc phase for that same nominal concentration and temperature, leading to

$$x_n = P_n(T)x_c^{\mathrm{Fmc}}(T) + [1 - P_n(T)]x_c^{\mathrm{AFmc}}(T). \quad (1)$$

Hence for nominal Si concentrations x_1 and x_2 we can derive the critical concentration of each phase by linear combination of Eq. (1) such that

$$x_c^{\mathrm{Fmc}}(T) = \frac{P_1(T)x_2 - P_2(T)x_1}{P_1(T) - P_2(T)}, \quad (2)$$

$$x_c^{\mathrm{AFmc}}(T) = \frac{[1 - P_2(T)]x_1 - [1 - P_1(T)]x_2}{P_1(T) - P_2(T)}. \quad (3)$$

For $PrMn_2Ge_{2-x}Si_x$ the width of the two-phase region is quite broad ($\delta x > 0.3$) from the AFl phase to the temperature where Pr orders, suppressing the AFmc phase by reinforcement of ferromagnetic interplanar coupling. This causes the boundaries of the two-phase region to shift sharply to higher Si concentration as is evident in Fig. 2.

Due to magnetostriction, what appears to be a region of coexistence of magnetic states in Fig. 2 could equally be seen as a phase gap, i.e., where a certain crystalline state is excluded by the magnetic exchange interaction which forces the lattice into one of two states (Fmc or AFmc). The onset (nucleation) of this region could be described as a *domino effect* mediated by lattice strain, such that the magnetostriction associated with the appearance of either of these states provides a positive feedback mechanism promoting further propagation of that state in the surrounding lattice. This leads us to consider the phase gap in terms of the average Mn-Mn nearest-neighbor

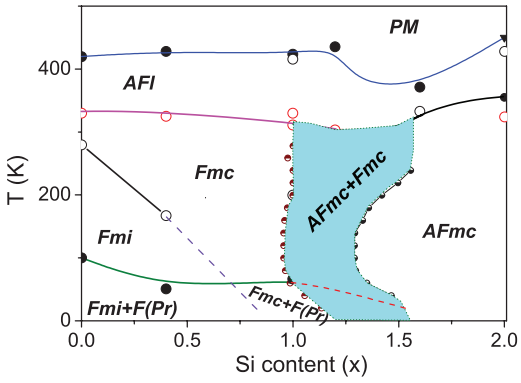

FIG. 2. (Color online) Magnetic phase diagram of $PrMn_2Ge_{2-x}Si_x$. Full symbol data are from Ref. 15. The boundary between Fmi and Fmc phases has been extrapolated (dotted line) into the region of ferromagnetic ordering of the Pr sublattice. Small symbols show the extrapolated boundaries of the two-phase region.

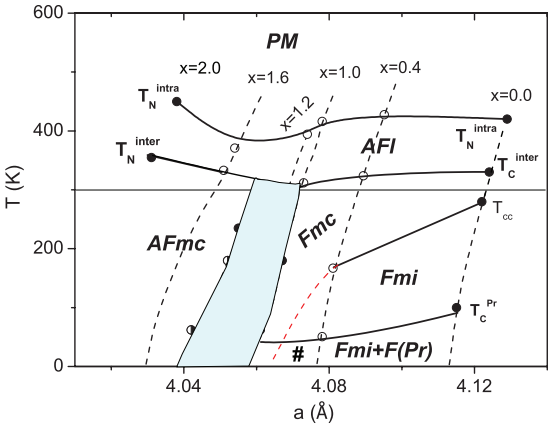

FIG. 3. (Color online) Magnetic phase diagram of $PrMn_2Ge_{2-x}Si_x$ as a function of a lattice parameter. Data for $x = 0$ and 2 come from Refs. 8 and 7, respectively. The shaded region shows the phase gap, the symbol # indicates coexistence of Fmc and F(Pr), and the dashed line shows the extrapolated boundary between Fmc and Fmi.

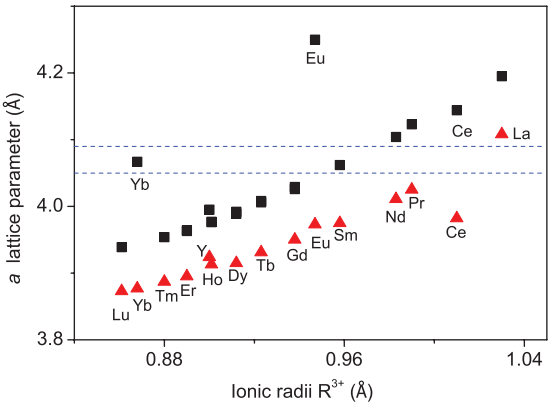

FIG. 4. (Color online) The room-temperature a lattice parameter of RMn_2X_2 compounds as a function of the R^{3+} ionic radius. Squares signify X = Ge and triangles signify X = Si. The two-phase region is broadly defined by the dashed lines as discussed in the text.

distance ($d^{\text{intra}}_{\text{Mn-Mn}} = a/\sqrt{2}$) by redrawing the phase diagram as a function of the a lattice parameter (shown in Fig. 3).

Figure 3 clearly demonstrates the existence of a "gap" (shown as a shaded region) between AFmc and Fmc. This gap is quite large ($\partial a/\bar{a} \approx 0.5\%$) and essentially temperature independent. The phase gap opens up at the transition from AFl (below which the axial component of magnetic order appears), and largely follows the line of thermal expansion, apart from minor shift due to ferromagnetic ordering of Pr.

Recalling the dependence of a lattice parameter on Si concentration, we expect larger lattice strain for concentrated solutions of Si and Ge (i.e., for $0.5 \leqslant x \leqslant 1.5$). We have examined peak widths of the (110) and (002) reflections, representing the strain in the a-b plane and c axis, respectively, for evidence of strain broadening. Although instrumental broadening dominates the measured peak widths, concentration-dependent lattice and magnetoelastic strain components can be identified. The former, which is independent of temperature, is seen in both (110) and (002) reflections while the latter is evident only in the (110) reflection, where additional peak broadening is seen only in the two-phase region. The high Si concentration range ($x \geqslant 1.2$) has the narrowest peaks, indicating the least amount of lattice strain, whereas the low Si concentration range ($x < 1.0$) shows significant lattice strain, with the highest value appearing close to equal concentrations of Ge and Si. Observation of larger strain at high Ge concentration indicates that chemical pressure from Ge is more critical than that from Si. Given the known sensitivity of Mn magnetic exchange interactions to Mn-Mn near-neighbor distances in RMn_2X_2 compounds,[2,17–19] the two-phase region is considered to derive from nonuniform distribution of Si and Ge, leading to different local magnetic environments. Whether the distribution of Ge and Si is random or nonrandom is unclear without further characterization. It is well known that binary metallic solutions (such as exist at the mixed site in pseudoternary RMn_2X_2 compounds) tend towards short-range chemical order,[35] and may even display considerable local lattice strain fields.[36,37] A nonrandom distribution involving short-range chemical order and local lattice strain seems likely; however, the possibility of a miscibility gap is not excluded.

Crystallite size can be seen in the Lorentz components of diffraction peaks. As noted above, instrumental broadening dominates the neutron diffraction peak widths of this study, so we cannot deduce anything about crystallite size. However, we are able to place a lower limit on crystallite size of $\sim$1 μm from x-ray diffraction.[38]

In light of this observation of the close dependence of the two-phase region on lattice size (specifically the a lattice parameter), and of the link with lattice strain, we have reviewed the broader family of RMn_2X_2 compounds for similar magnetic and structural behavior, paying particular attention to the pseudoternaries (for which lattice strain is expected to be enhanced) for indications of the coexistence of AFmc and Fmc phases. Figures 4 and 5 summarize our review of available data.[6,10,15,18,24,27–34,39]

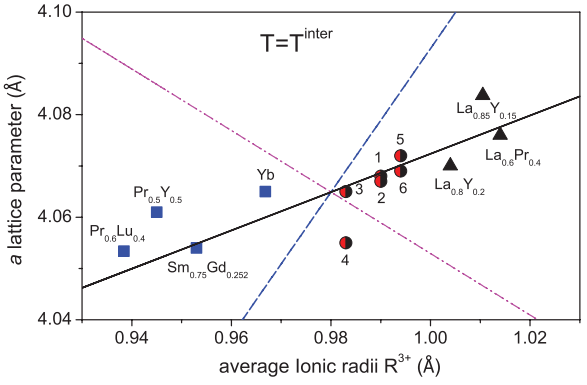

FIG. 5. (Color online) The a lattice parameter at the critical temperature of the two-phase region versus average ionic radius of the rare-earth ion for $R_{1-y}R'_yMn_2X_2$ compounds. Squares indicate germanides, triangles indicate silicides, and bisected circles indicate a mixture of Ge and Si. Lines indicate expected trends due to variation of the rare-earth ion (dashed line), the metalloid ion (dot-dash line), and a weighted combination of the two (solid line). 1: $PrMn_2Ge_{1.0}Si_{1.0}$; 2: $PrMn_2Ge_{0.8}Si_{1.2}$; 3: $NdMn_2Ge_{1.2}Si_{0.8}$; 4: $NdMn_2Ge_{1.0}Si_{1.0}$; 5: $CeMn_2Ge_{1.0}Si_{1.0}$; and 6: $CeMn_2Ge_{0.8}Si_{1.2}$.

Figure 4 plots the a lattice parameter at room temperature against average radius of the rare-earth ion (nominally R^{3+}) for all ternary $R\mathrm{Mn_2}X_2$ compounds. We note that all $R\mathrm{Mn_2Ge_2}$ compounds have a larger a lattice parameter than their $R\mathrm{Mn_2Si_2}$ counterparts. This is a direct consequence of the increased chemical pressure of the larger Ge ion. Moreover, the general monotonic increase of the a lattice parameter with radius of the rare-earth ion demonstrates the importance of chemical pressure of the rare-earth ion. Figure 4 also shows that $\mathrm{YbMn_2Ge_2}$, $\mathrm{EuMn_2Ge_2}$, and $\mathrm{CeMn_2Si_2}$, where the rare-earth ion is thought to be in a mixed valence state,[17] do not follow the monotonic trend of the other compounds.

We now focus on the region between the dashed horizontal lines of Fig. 4, which roughly defines the a lattice parameter of those compounds for which we have found published evidence of a two-phase region. Figure 5 plots the a lattice parameter at the critical temperature where the two-phase region appears (equivalent to T_N^{inter} and T_C^{inter} in Fig. 3) versus average radius of the rare-earth ion (nominally R^{3+}). All compounds in Fig. 5 are pseudoternaries, i.e., compounds in which we expect enhanced lattice strain due to local variations in concentration of the species on the mixed lattice site. For the purpose of this discussion we also include compounds with mixed-valence rare-earth ions: $\mathrm{YbMn_2Ge_2}$, where Yb has mean valence 2.35,[17] and $\mathrm{CeMn_2Ge_{1.0}Si_{1.0}}$ and $\mathrm{CeMn_2Ge_{0.8}Si_{1.2}}$, where we estimate Ce has mean valence 3.12.

Three of the four possible series of pseudoternary compounds are represented here: the $R_{1-y}R'_y\mathrm{Mn_2}X_2$, $R\mathrm{Mn_2}X_{2-x}X'_x$, and $R^{n+}_{1-y}R^{3+}_y\mathrm{Mn_2}X_2$ series, where $n = 2$ for Yb and $n = 4$ for Ce. We find no evidence of phase separation in available data on pseudoternary $R\mathrm{Mn_{2-x}}T_xX_2$ compounds including $\mathrm{PrMn_2Fe_{2-x}Ge_2}$[13] (for which Fe substitution causes lattice contraction and a transition from Fmc to AFmc, but no two-phase region).

We note the monotonic increase in a lattice parameter with ionic radius of the rare-earth ion across the series, and that germanides are grouped at the lower left of Fig. 5 while silicides are grouped at the upper right with mixed metalloids (Ge + Si) in the midrange. This indicates a close and consistent dependence of the critical limit in Mn-Mn magnetic exchange on the combination of chemical pressure from the R and X sites. Confirmation of this dependence is indicated by the three lines that overlie the data points in Fig. 5. These lines show the dependence of a lattice parameter on three variables: average radius of the rare-earth ion (dashed line), average radius of the metalloid ion (dot-dash line), and a weighted contribution of both components (solid line). The slopes of the lines representing the average contribution from rare-earth and metalloid sites were extracted from Fig. 4. The slope of the line representing the weighted contribution from both sites reflects the mean chemical pressure, and is in good agreement with the trend of observed data. The weighting takes account of the fact that the difference in ionic radii of Si and Ge exceeds the difference between extremes in ionic radii of the rare-earth ions plotted in Fig. 5. This line represents the critical pressure for stabilization of a single phase, beyond which phase separation occurs due to spontaneous magnetostriction resulting from the interplay between local strain fields and the Mn-Mn magnetic exchange interaction.

Recalling that planes of X atoms interleave planes of both rare-earth atoms and Mn, it is curious that chemical pressure from the rare-earth plane should have the same consequence on the Mn-Mn intraplanar exchange as that from the X plane. Magnetic strain broadening visible in the (110) reflection suggests that magnetic strain is resolved in the a-b plane, through a distribution of intraplanar Mn-Mn spacings. Conversely its apparent absence in the (002) reflection suggests lower axial magnetic strain, belying the observation that chemical pressure from R ion distributions produces two-phase behavior. High-resolution scattering studies are needed to accurately determine strain distributions, domain sizes, and the role of atomic and magnetic short-range order.

In summary, we have produced a new phase diagram for $\mathrm{PrMn_2Ge_{2-x}Si_x}$, thereby identifying the spontaneous magnetostriction that propagates phase separation, and mapped out the boundaries of the two-phase region. We have shown how this region depends on lattice parameter, chemical pressure from the rare-earth and metalloid sites, and lattice strain. Our results provide valuable insights into the magnetostructural correlations of this series, providing a basis for review of the magnetostructural correlations across the whole family of $R_{1-y}R'_y\mathrm{Mn_2}X_{2-x}X'_x$ compounds. Our findings and related analyses can be used to accurately predict whether pseudoternary $R_{1-y}R'_y\mathrm{Mn_2}X_{2-x}X'_x$ compounds will form Fmc, AFmc, or mixed Fmc + AFmc phases, based on the compositions of R and X and on lattice parameter.

The work is supported in part by grants from the Australian Research Council by Discovery Grants (DP0879070 and DP110102386) and LIEF Grant (LE0775559) and from the Access to Major Research Facilities Programme which is a component of the International Science Linkages Programme established under the Australian Government's innovation statement. We also thank Dr. A. Arulraj and Dr. N. Stusser for their help during the neutron experiments at BER II, Lise-Meitner Campus, Helmholtz-Zentrum Berlin and Dr. Andrew Studer for his help during the neutron experiments at Wombat of OPAL, ANSTO.

*sjk@ansto.gov.au

[1] A. Szytula, in *Handbook of Magnetic Materials*, edited by K. H. J. Buschow (Elsevier, Amsterdam, 1991), Vol. 6, Chap. 2.

[2] J. L. Wang, S. J. Campbell, A. J. Studer, M. Avdeev, R. Zeng, and S. X. Dou, J. Phys.: Condens. Matter **21**, 124217 (2009).

[3] A. Szytula and S. Siek, J. Magn. Magn. Mater. **27**, 49 (1982).

[4] H. Fujii, M. Isoda, T. Okamoto, T. Shigeoka, and N. Iwata, J. Magn. Magn. Mater. **54–57**, 1345 (1986).

[5] G. Venturini, R. Welter, E. Ressouche, and B. Malaman, J. Magn. Magn. Mater. **150**, 197 (1995).

[6] M. Hofmann, S. J. Campbell, and S. J. Kennedy, J. Phys.: Condens. Matter **12**, 3241 (2000).

[7]S. J. Kennedy, T. Kamiyama, K. Oikawa, S. J. Campbell, and M. Hofmann, Appl. Phys. A **74**, S880 (2002).
[8]I. Dincer, Y. Elerman, A. Elmali, H. Ehrenberg, and G. André, J. Magn. Magn. Mater. **313**, 342 (2007).
[9]E. Duman, M. Acet, I. Dincer, A. Elmali, and Y. Elerman, J. Magn. Magn. Mater. **309**, 40 (2007).
[10]J. L. Wang, A. J. Studer, S. J. Campbell, S. J. Kennedy, R. Zeng, and S. X. Dou, IEEE Trans. **47**, 2893 (2011).
[11]S. Siek and A. Szytula, J. Phys. **40**, C5 (1979).
[12]G. Venturini, B. Malaman, and E. Ressouche, J. Alloys Compd. **237**, 61 (1996).
[13]J. L. Wang, S. J. Campbell, A. J. Studer, M. Avdeev, M. Hofmann, M. Hoelzel, and S. X. Dou, J. Appl. Phys. **104**, 103911 (2008).
[14]G. Liang and M. Croft, Phys. Rev. B **40**, 361 (1989).
[15]S. Kervan, A. Kilic, and A. Gencer, J. Phys.: Condens. Matter **16**, 4955 (2004).
[16]J. L. Wang, S. J. Campbell, R. Zeng, C. K. Poh, S. X. Dou, and S. J. Kennedy, J. Appl. Phys. **105**, 07A909 (2009).
[17]M. Hofmann, S. J. Campbell, and A. J. V. Edge, Appl. Phys. A **74**, S713 (2002).
[18]M. Hofmann, S. J. Campbell, and A. V. J. Edge, Phys. Rev. B **69**, 174432 (2004).
[19]P. Kumar, K. G. Suresh, A. K. Nigam, A. Magnus, A. A. Coelho, and S. Gama, Phys. Rev. B **77**, 224427 (2008).
[20]A. Szytula and I. Szott, Sol. Stat. Comm. **40**, 199 (1981).
[21]I. Nowik, Y. Levi, I. Felner, and E. R. Bauminger, J. Magn. Magn. Mater. **147**, 373 (1995).
[22]R. Welter, G. Venturini, E. Ressouche, and B. Malaman, J. Alloys Compd. **218**, 204 (1995).
[23]S. Di Napoli, A. M. Llois, G. Bihlmayer, and S. Blügel, Phys. Rev. B **75**, 104406 (2007).
[24]J. L. Wang, S. J. Campbell, S. J. Kennedy, M. Hofmann, R. Zeng, S. X. Dou, A. Arulraj, and N. Stusser (unpublished).
[25]J. Rodriguez-Carvajal, FULLPROF, http://www-llb.cea.fr/fullweb.
[26]A. E. Clark, J. R. Cullen, O. D. McMasters, and E. R. Callen, AIP Conf. Proc. **29**, 192 (1976).
[27]D. Rossi, R. Marazarra, D. Mazzone, and R. Ferro, J. Less Common Metals **59**, 79 (1978).
[28]H. Fujii, T. Okamoto, T. Shigeoka, and N. Iwata, Solid State Commun. **53**, 715 (1985).
[29]M. Duraj, R. Duraj, and A. Szytula, J. Magn. Magn. Mater. **79**, 61 (1989).
[30]Y. Q. Jia, J. Solid State Chem. **95**, 184 (1991).
[31]G. Venturini, B. Malaman, and E. Ressouche, J. Alloys Compd. **240**, 139 (1996).
[32]Y.-G. Wang, F. M. Yang, C. P. Chen, N. Tang, and Q. D. Wang, J. Phys: Condens. Matter **9**, 8539 (1997).
[33]Y.-G. Wang, F. M. Yang, C. P. Chen, N. Tang, and Q. D. Wang, J. Alloys Compd. **257**, 19 (1997).
[34]S. Okada, K. Kudou, T. Mori, K. Iizumi, T. Shishido, T. Tanaka, and Peter Rog, J. Cryst. Growth **244**, 267 (2002).
[35]S. J. Kennedy and T. J. Hicks, J. Magn. Magn. Mater. **81**, 56 (1988).
[36]H. Reichert, V. N. Bugaev, O. Shchyglo, A. Schöps, Y. Sikula, and H. Dosch, Phys. Rev. Lett. **87**, 236105 (2001).
[37]P. Singh and S. Prakash, Phys. Rev. B **59**, 14226 (1999).
[38]J. L. Wang (unpublished).
[39]D. H. Ryan, J. M. Cadogan, and A. V. J. Edge, J. Phys.: Condens. Matter **16**, 6129 (2004).